THE STIFFNESS OF POLYMERS IN RELATION TO THEIR STRUCTURE

L. HOLLIDAY* and J. W. WHITE†

Physical Chemistry Laboratory, South Parks Road, Oxford, UK.

ABSTRACT

In this paper we set out to review experimental values and theoretical estimates of the Young's modulus of crystalline and amorphous polymers. Not unnaturally, this reveals a lack of complete numerical agreement. The disparity is worst for the transverse directions to the fibre axis when calculated theoretically. Nor is there complete agreement between experimental determinations of the moduli made by different experimental techniques. Nevertheless, an interesting and reasonably satisfactory picture emerges from which can be seen those areas which are most in need of further research.

After outlining the problem in general, we give an account of the various methods available for obtaining the Young's modulus of polymers along the chain and at right angles to the chain. These consist of macroscopic stretching methods, the use of sound waves, x-ray diffraction, Raman scattering and inelastic neutron scattering spectroscopy. The relative significance of static and dynamic measurements is also discussed.

An account is given of experimentally determined values of $\mathbf{E}_{\parallel}$, the modulus along the chain, and in the next section these values are compared with theoretical estimates. It turns out that most work has been done with polyethylene, where major discrepancies can be seen between the experimental and theoretical values. However, other polymers have received a fair amount of attention.

Experimentally determined values of $\mathbf{E}_{\perp}$ are next discussed, and are compared with theoretical estimates. The situation here is confused, but largely because $\mathbf{E}_{\perp}$ has received less attention than $\mathbf{E}_{\parallel}$. Finally the problem of isotropic amorphous and crystalline polymers is considered. This is the most complicated, and technologically the most important. Some progress has been made in estimating theoretically Young's modulus from consideration of molecular stretching mechanisms, but basically the subject is still in its infancy.

1. INTRODUCTION

In virtually all applications of polymers, we are interested in one or more of three basic mechanical properties—stiffness, strength and toughness. Stiffness represents resistance to deformation, strength represents the ultimate load of stress which a material can withstand before it fails by fracture or excessive deformation, and toughness represents the work required to fracture a material. Of these three properties, stiffness is perhaps the most

* Department of Polymer Science, Brunel University.

† Department of Physical Chemistry, Oxford University.

basic, since there is a broad relationship between stiffness and strength in the ideal case. For example, as Vincent[1] has pointed out, one cannot expect to reach the theoretical strength before reaching the theoretical modulus. It is with the elastic modulus or stiffness that we are concerned in this paper. As a measure of stiffness, we shall use Young's modulus defined in the usual way

$$E = \sigma/\varepsilon$$

where E is Young's modulus, σ is stress, and ε denotes strain. This equation is valid for small strains, say less than one per cent. Since E is dependent upon the rate of strain, we shall define E as the limiting value, as the rate of strain tends to zero. Unless otherwise specified, we restrict ourselves to this limiting, or static, value.

Isotropic polymers have a single value of E and in this case the well-known relationship between the four elastic constants E (Young's modulus), G (shear modulus), K (bulk modulus) and ν (Poisson's ratio) apply.

$$E = 3G/(1 + G/3K) \tag{1}$$

$$G = E/2(1 + \nu) \tag{2}$$

$$K = E/3(1 - 2\nu) \tag{3}$$

For anisotropic polymers, there are more elastic constants, depending on the direction of test. For example, for uniaxially aligned chains, with which this paper is mainly concerned, there are at least two values of E; $E_{\parallel}$ and $E_{\perp}$, these being the values of E parallel and perpendicular to the chain direction. In materials of greater anisotropy, a fuller description of the stress/strain relationship is required[2,3]. For crystalline polymers, moduli can sometimes be obtained parallel to three or more crystallographic directions. The best known example of this is linear polyethylene, discussed below. These moduli are indicated by the symbol E_{hkl}, where hkl are the Miller indices of the plane perpendicular to the direction of modulus measurement. Alternatively for orthorhombic polyethylene the symbols E_a, E_b and E_c are used, E_c being the modulus in the chain direction.

Values of elastic modulus will be given in multiples of 10^{10} dyne cm^{-2}, which is the most convenient for comparison purposes. The relationships given by equations 4, 5 and 6 convert dyne cm^{-2} to other units:

S.I.	1 Newton metre^{-2}	$= 1\,\mathrm{N\,m^{-2}} = 10\,\mathrm{dyne\,cm^{-2}}$	(4)
Practical	1 Kg cm^{-2}	$= 10^6\,\mathrm{dyne\,cm^{-2}}$	(5)
	1 lb in^{-2}	$= 6.85 \times 10^4\,\mathrm{dyne\,cm^{-2}}$	(6)

In this paper we discuss first the various methods which have been used to measure the modulus in the chain direction and transverse to the chain. In the case of a fibre for example, the modulus in the chain direction should not be confused with the overall modulus along the fibre axis. It is the modulus within the crystalline regions in the fibre, determined in the direction of chain alignment and is therefore higher than the fibre modulus. It will be seen that there is a lack of agreement between values of modulus determined by different experimental methods. The values of the modulus

obtained macroscopically (e.g. with a tensile testing machine) differ from those obtained microscopically (e.g. by the shift in x-ray diffraction peaks under load or by inelastic neutron scattering spectroscopy, abbreviated to INSS).

We discuss secondly the way in which the experimentally determined values compare with a range of theoretical calculations, based on an assessment of the intra- and inter-molecular forces. There is a disparity between values in both cases—both in the crystallographic directions along the fibre axis and perpendicular to it. The discrepancy between theory and practice in the case of the transverse moduli reflects the position in other molecular crystals, where a knowledge of intermolecular forces and their range is fairly meagre.

Finally, we deal with the elastic modulus in isotropic, polycrystalline or amorphous polymers and how this may be estimated according to various models, from the longitudinal and transverse moduli obtained on crystalline polymers.

2. EXPERIMENTAL METHODS OF OBTAINING ELASTIC MODULI

The chief methods of measuring the elastic constants of crystals, and hence their elastic moduli, are by macroscopic stretching, sound velocity measurements, measurements of the shift in x-ray reflections under an applied stress, Raman scattering spectra and by INSS. An important aspect of these different methods is that they give data on the crystal elasticity at different levels of scrutiny. By this, we mean that the size of the deformation observed is progressively lower in passing from method to method, so that the property of crystalline regions only is ultimately measured. For most pure single crystals of uniform texture it is to be expected that the measurements of elastic constants for a crystal will be independent of which of the above methods has been chosen and this seems to be true for single crystals of argon, for example[4, 5]. For polymers, one may expect revealing differences from measurements made by the several methods because of their mosaic texture and because the dynamic studies (sound wave and phonon measurements) may be restricted to studying either isothermal or adiabatic sound propagation[6]. It is normally observed in polymer physics that Young's modulus measured by a dynamic method is greater than the corresponding static value, i.e. $E_{dyn.} > E_{stat.}$. Whilst this is true for polycrystalline materials which are normally studied, it need not be true for single crystals or measurements which are restricted to single crystal regions. There are circumstances where $E_{dyn.} = E_{stat.}$ and this point will be discussed later, since otherwise it may give rise to confusion.

We shall now discuss briefly the various techniques for determining E, with comments on the way in which a particular technique can bias results.

Macroscopic stretching method

This method requires little discussion, since it is so well known. The exact size and form of the test material is a matter of convenience and film, strip or fibre may be used. If an anisotropic material is required, it will be

oriented and stabilized in the usual way (see, e.g., ref. 2). If an isotropic sample is required, care must be taken not to stretch or otherwise orient the material inadvertently during sample preparation. Strain rates are low. Bulk measurements of this kind are of intrinsic interest for the application of polymers in industry, but what is noteworthy is that the values obtained for the Young's modulus are usually an order of magnitude lower than those calculated or obtained by more 'microscopic' measurements. The comparison of microscopic and macroscopic measurements permits the evaluation of aggregate theories for the calculation of bulk polymer properties (see, e.g., ref. 7).

Sound wave measurements

The transverse modulus for polypropylene determined from sound velocity studies is reported at 4.04×10^{10} dyne cm^{-2} [8]. This may be compared with the bulk measurements of 2.3×10^{10} dyne cm^{-2} and the x-ray value of approximately 3.0×10^{10} dyne cm^{-2} at 28°C. There are only a few measurements of this kind for polymers although the method has been extensively applied to molecular crystals, and recently to inert gas atomic crystals[3].

The technique is in principle quite simple, and one modification consists in measuring the transit time, around (10 μs), for 10 MHz ultrasonic power in a narrow pulse to travel from the transducer through the substrate and return. Quartz transducers may be used for this work and must be strongly bonded into the samples. The pulses and their time separation may be simply observed using an oscilloscope. Since quite small transducers may be obtained, the elastic constants in different crystalline directions can be readily measured. Difficulties arise in practice because of faulty bonding between the crystal and the transducer and through specimen attenuation. The crystal size must be measured in the transmission direction.

For a non-homogeneous sample with many disordered crystalline blocks, as in many polymer specimens, considerable difficulties can be anticipated due to reflections from grain boundaries. The spatial range of the measurement is such that the sound velocity obtained is more characteristic of the polycrystalline average than of a true crystallite direction. The relations between single crystal and polycrystalline velocities have been discussed by Hill[9]. It is conceivable that for highly crystalline, highly oriented samples, many interesting data could be obtained by this method.

X-Ray determinations of crystalline elastic moduli

This method, largely developed by Sakurada and his colleagues[10], depends on observing the shift under a static stress of the characteristic x-ray diffraction spots associated with periodic structures in the polymer. These shifts were noted by Baker and Fuller[11] in 1943, although they did not calculate elastic moduli. This was first done by Dulmage and Contois[12] who measured the extension of the fibre identity period (FIP) for eight polyesters and polyesteramides.

A full description of the experimental arrangements necessary to do the measurements has been given[13] in the context of measurements on polyvinyl alcohol, polyethylene, polypropylene, polyoxymethylene, cellulose and polyvinylidene chloride. The specimens were highly oriented filaments or

fibres prepared by dry spinning or extrusion. They were stretched under constant load in a special sample jig fitted to the x-ray camera, as shown in *Figures 1* and *2*. The specimen length was *ca.*35mm and the specimen

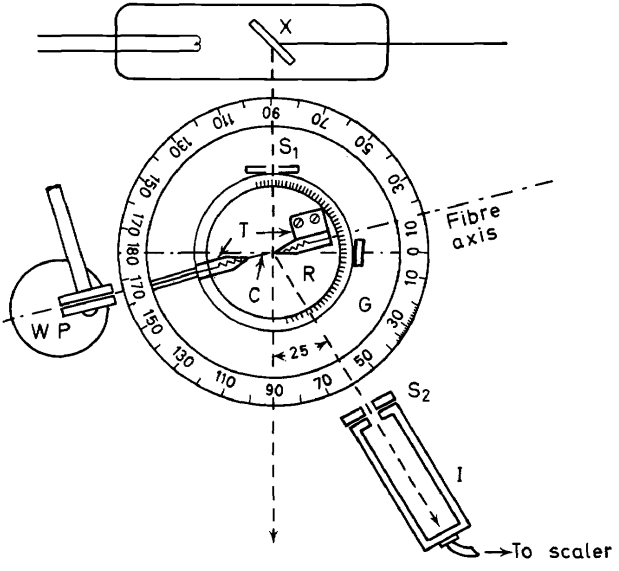

Figure 1. The x-ray diffractometer with stretching mechanism: (X) x-ray tube; (I) Geiger–Müller counter; (S_1), (S_2) slit system; (C) specimen; (T) stretching clamps; (P) pulley; (W) weight; (G) goniometer; (R) specimen rotor [After Sakurada, Nukushina and Ito[13]].

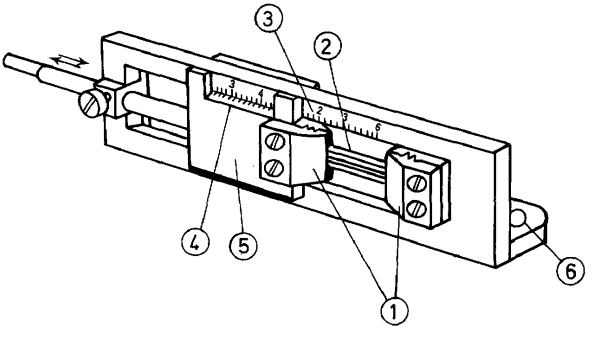

Figure 2. Stretching mechanism: (1) clamps; (2) fibre specimen; (3) rule; (4) Vernier; (5) slide; (6) screw hole [After Sakurada, Nukushina and Ito[13]].

extension could be read to 0.03 mm. Usually a meridional reflection was chosen and experimental error in measuring the shift of its maximum intensity was approximately ± 1 minute of arc. This corresponds to 2.5×10^{-4} Ångströms so that the lattice extension could be measured by approximately 0.02 per cent.

The stress, σ, may be calculated from the weight applied to the specimen (at constant load) and calculated cross-sectional area of the specimen (the latter corrected for elongation). The elastic modulus is calculated from the expression:

$$\sigma = E\varepsilon \tag{7}$$

given that

$$\varepsilon = (\Delta d/d_0) \tag{8}$$

where d_0 is the distance between planes before applying the stress and Δd is the change in distance under stress.

It can be seen that this method is one of the most accurate available for measuring the elastic moduli of the crystalline regions in polymers. Intrinsic accuracy is limited only by the practical ability to measure the shift in diffraction maximum and by the method of calculating the stress applied to the crystalline element. Here it is necessary to make the assumption of a series model for applying the external forces to the crystalline polymer segments. This assumption of homogeneous stress is a possible weakness of the method, and much effort has been devoted to establishing its validity. One method of check has been to try to show that the elastic modulus in the chain direction is the same when measured by this method for different samples of the same material[14]. For example, for polyethylene different samples gave a lattice modulus measured by x-rays of 240, 240, 230 $\times$ 10^{10} dyne cm^{-2}, the bulk specimen moduli for the same materials being 2.4, 15, 3.1 $\times$ 10^{10} dyne cm^{-2}. In another example, the lattice modulus of polyvinyl alcohol measured in the dry and wet (swollen) states, was found to be the same although the specimen (bulk) modulus changed by a factor of 100 under this treatment. Later work[10] has tended to confirm this view of homogeneous stress, since polymers with different fine textural structures have the same lattice moduli. The data for these different materials all fall upon the same stress/strain curve as determined by x-rays. These curves often have two straight line regions (*Figures 3, 4*) which may indicate a different mode of deformation at high extensions.

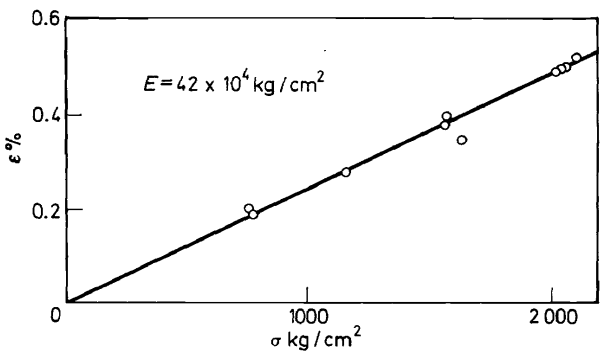

Figure 3. Stress/strain curve for polypropylene lattice [After Sakurada, Nukushina and Ito[13]].

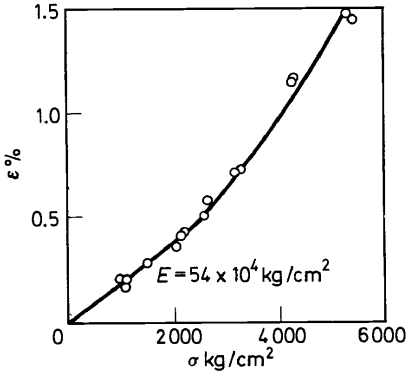

Figure 4. Stress/strain curve for polyoxymethylene lattice [After Sakurada, Nukushina and Ito[13]]

The overall moduli of the specimens are always found to be much lower than the lattice moduli in the direction of the chain axis. This indicates to what extent the moduli in the amorphous regions are lower than those for the crystalline regions. Even in the chain direction, however, it is not clear that all factors which could violate the assumption of homogeneous stress have been discovered and eliminated.

In the transverse direction, the assumption of homogeneous stress is even more a source of concern. This is partly because the moduli associated with the interchain interactions (E_a and E_b for example in polyethylene) are much more isotropic and are numerically closer to the values supposed for moduli in the amorphous fraction. Since theoretical estimates for these directions are still in disagreement, new methods of measuring the true crystalline modulus are essential to further discussion. There is some evidence that an assumption of homogeneous strain may be better for interpreting x-ray data[7] in the *a* direction.

Raman scattering measurements

When a monochromatic beam of light enters a colourless solid, liquid or gas, a small fraction (say 1/1000 of the intensity is scattered by the molecules. Energy analysis of the scattered light, with a monochromater, reveals that most of the scattered intensity appears at the same energy as the incident line (elastic or Rayleigh scattering). A small fraction appears at energies differing from the incident line by quanta of molecular vibrational or rotational energy. This is the inelastic or Raman scattering. As the energy transfer can be easily measured with modern spectrographs, Raman scattering is a good method of measuring molecular vibration and rotation frequencies subject to the limitations imposed by optical selection rules[15] and by sampled turbidity and fluorescence. Laser sources have greatly reduced the latter problems which are acute in polymer specimens. The applications for polymer spectroscopy have been reviewed recently[16, 17].

To measure the elastic modulus of a hydrocarbon chain it is necessary to identify the vibration frequencies of the 'accordion' like motion of the

planar zig-zag chain. This motion is quantized and the lowest frequency oscillation involves the two chain ends moving parallel to the axis with maximum amplitude with the chain centre at rest. The wavelength of the standing wave of this frequency is just twice the chain length ($2L$) since the two ends are moving 180° out of phase. Higher modes of vibration charac-

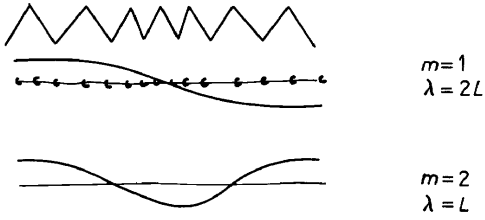

terized by more modes along the chain and mode numbers $m = 2, 3 \ldots$ may occur as shown above. The highest frequency occurs when neighbouring atoms are moving 180° out of phase. By knowing the frequency ν_m of these waves (from the Raman) and their wavelength, λ_m, the velocity of sound, v, is calculated, $v = \nu_m \lambda_m$. Using the relationship

$$v = (E/\rho)^{\frac{1}{2}} \tag{9}$$

where E is Young's modulus and ρ the chain density, the modulus can be calculated.

In 1949 an estimate of the elastic modulus of polyethylene was made using this method by Mizushima and Shimanouchi[41], who observed the lowest frequency Raman active chain vibrations of a number of alkanes. They used the assumption implicit above that the hydrocarbon molecule could be treated as a uniform elastic rod, giving the following relationship for $E_{\parallel}$

$$E_{\parallel} = \{(2L/m)\nu_m\}^2 \rho \tag{10}$$

Having observed only the frequency for $m = 1$ they used chains of different length, L, to verify the relation and obtained a value for $E_{\parallel}$ of 340×10^{10} dyne cm^{-2}. It is fortunate that the argon ion laser has made it possible to extend this Raman work by revealing more of the longitudinal modes, ν_m, of vibration for hydrocarbon molecules. Using this device, Shauffele and Shimanouchi[42] obtained a recent estimate of the elastic modulus of an infinite polyethylene chain as $358 \pm 25 \times 10^{10}$ dyne cm^{-2}. A simplified view of the connection of these modulus measurements with those of inelastic neutron scattering spectroscopy has recently been given[43] by White.

Figure 5 shows the Raman spectrum from solid $C_{36}H_{74}$ at 300°K. The Rayleigh line appears with great intensity at energy transfer $hc\,\Delta\tilde{\nu} = 0$; ($h$ is Planck's constant, c the velocity of light). The laser excitation is particularly valuable here because of the narrow width of the exciting line. The sharp peaks separated by 67.4, 189, 303 etc., cm^{-1}, from $\Delta\tilde{\nu} = 0$ correspond to values of $m = 1, 3, 5$ etc. for the chain longitudinal acoustic 'accordion' mode. Bands for even m are excluded because of optical selection rules and

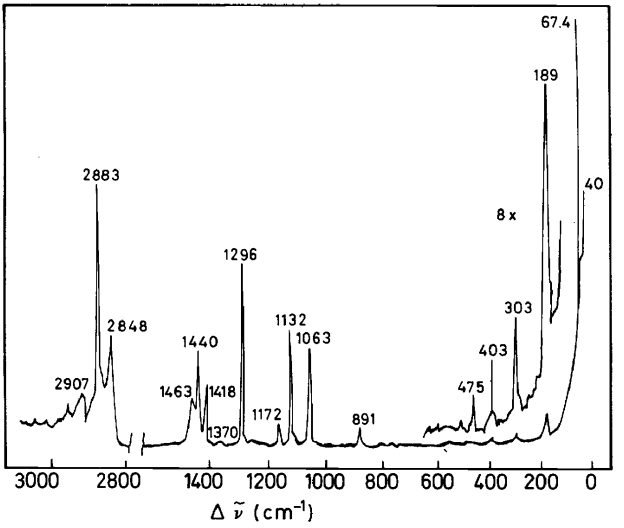

Figure 5. Raman scattering by crystalline $C_{36}H_{74}$(300°K) [After Shauffele and Shimanouchi[42]].

the frequencies observed above 1000 cm^{-1} are localized intramolecular deformations, some possibly showing the effects of dispersion in their shapes.

Shauffele and Shimanouchi[42] showed that the frequencies for a large number of hydrocarbons and mode numbers all fit on to the same curve (*Figure 6*). This diagram has several important consequences. The abscissa, m/n, measures the phase shift between the amplitudes of neighbouring atoms and is inversely proportional to the 'wavelength' of the mode, m. The figure is thus a dispersion curve[43] relating frequency and wavevector in the mode.

It can be seen that for long waves (m/n small) the approximation of a uniform elastic rod is good. The slope gives the velocity of sound and hence the elastic modulus. The deviations at higher frequency (for shorter waves) are very similar to the dispersion phenomena found for lattice vibrations[18].

That points for many different hydrocarbons fit the same curve illustrates the validity of transferring the force field from one to another and, as an ultimate extension, to polyethylene. Because the chain lengths in polymer segments are long and because of their spread of values it may be difficult to observe the longitudinal Raman modes like *Figure 5* directly. One report of this has been made[15] which indicates extensive and reproducible chain folding. Shauffele and Shimanouchi predict that the separation of lines for $m = 1, 3$ etc., should be *ca.* 10^{-2} cm^{-1} for polyethylene.

Inelastic neutron scattering measurements

Raman scattering spectroscopy measurements of the paraffin chain modulus were made possible because both the wavelength and frequency of the chain vibrational mode were known or came from spectra. Inelastic neutron scattering spectroscopy, INSS, also has this feature and in addition

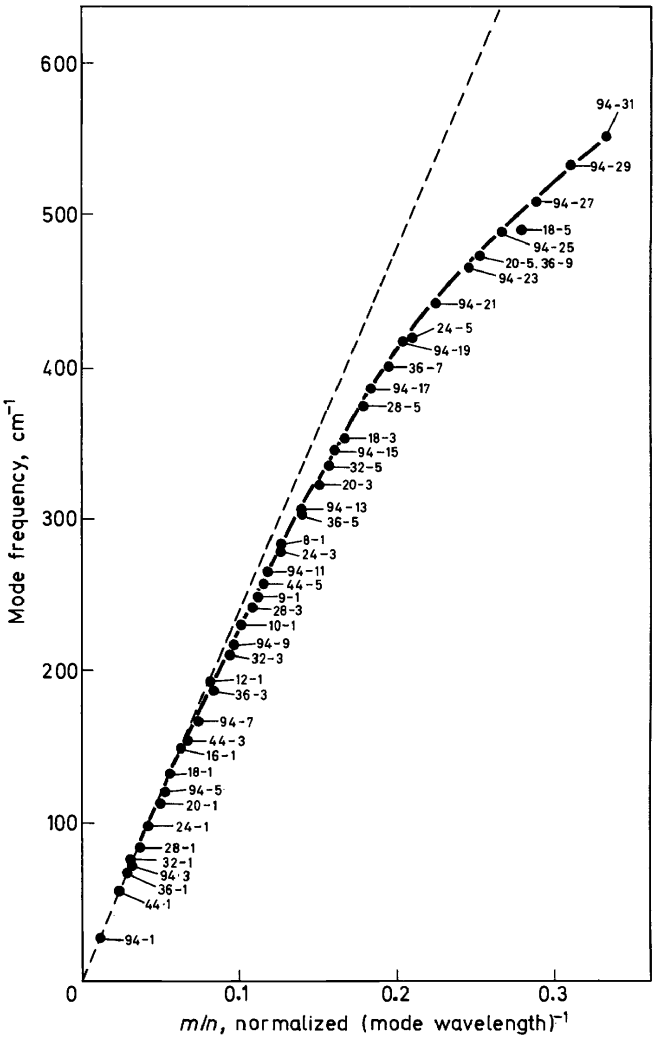

Figure 6. Low-frequency Raman bands plotted as a function of m/n and their assignments n-m. (--- shows theoretical line for a uniform elastic rod [After Shauffele and Shimanouchi[42]].

the remarkable ability to selectively measure modes of prechosen frequency and wavevector (h/λ_m) in a chosen crystallographic direction. Dispersion curves, and hence the elastic constants, have been measured revealing the subtleties of the distance dependence of force laws in single crystals of metals, ionic salts, semiconductors and most recently molecular crystals[18–20]. This type of information is potentially accessible for polymers but the chief difficulty, until recently, has been to find neutron methods applicable to materials with such poor crystalline mosaic spreads as polymers have, even when oriented.

INSS[18] has made, and will make, important contributions to the study of

polymer motions by revealing the phonon density of states spectrum of the chain and lattice vibrations[21,22] for comparison with theory and specific heats[22]. It has also identified other optically forbidden modes in polymers. Methyl torsion vibrations[23] appear particularly strongly and other side group motions may be equally tractable.

For determining the nature of the polymer binding forces, in and perpendicular to the chains coherent inelastic neutron scattering must play a dominant role. A simple sketch of the method and its relation to other spectroscopy has been given[43]. We will concentrate here on the two methods which have so far successfully determined the elastic moduli parallel and perpendicular to the chain in polyethylene and polytetrafluorethylene. The wider question of the shape of the dispersion curves and the range of the forces causing the modulus will be treated elsewhere[24,25] with more details of the experimental method suitable for polycrystals.

Theory of the neutron method

The neutron is uncharged and interacts with matter quite differently from light or charged particles. Secondly because neutrons are massive there are appreciable transfers of momentum as well as energy when excitation by neutrons occurs. For polymers the first point allows excitation of optically forbidden molecular transitions and the second makes it possible to observe lattice vibrations whose 'momentum' or wavevector is both variable and well away from the Brillouin zone centre as required for optical spectra.

As a result, molecular neutron scattering by contrast with the Raman effect is often strongly angular dependent and the quantity of interest for measurement is the double differential scattering cross section $\partial^2\sigma/\partial\Omega\partial\omega$. This measures the intensity of scattering into solid angle element $\partial\Omega$ for energy charge $\hbar\,\partial\omega$ where $\hbar = h/2\pi$. For a highly monochromatic incident beam this cross section represents the intensity of the scattered spectrum and is given by [19,20]

$$\frac{\partial^2\sigma_{\text{coh}}}{\partial\Omega\,\partial\omega} = \hbar \times \frac{(2\pi)^3}{V} \times \sum_{\mathbf{q},s} \frac{k}{k_0} \times \delta(\hbar\omega \mp \hbar f) \times \sum_{\boldsymbol{\tau}} \delta(\mathbf{Q} \mp \mathbf{q} - 2\pi\boldsymbol{\tau})$$
$$\times \frac{\hbar(n + \frac{1}{2} \pm \frac{1}{2})}{2f} \times \frac{\left|\sum_l \bar{b} \exp\left[i\mathbf{Q} \cdot \boldsymbol{\rho}_l\right] \times \mathbf{Q} \cdot \mathbf{U}^l\right|^2}{M_l} \times \exp - [2W_l] \qquad (11)$$

where V is the volume of the crystal and the first sum is over modes s of wavevector $\mathbf{q}$ and frequency f. The sum over reciprocal lattice vectors $\boldsymbol{\tau}$ shows that the cross section is greatest near diffraction peaks and especially when the vector condition in the delta function is satisfied. The final sum is over atoms, mass M_l, in the unit cell, distinguished by vectors, $\boldsymbol{\rho}_l\mathbf{U}^l$ is the polarization vector for the *lth* atom's displacement in the mode s of wavevector $\mathbf{q}$, and $\exp - [2W_l]$ is the Debye–Waller factor. $\mathbf{Q}$ is the momentum transfer (see equation 13).

For a single scattering atom this general expression can be reduced to

$$\frac{\partial^2\sigma_{\text{coh}}}{\partial\Omega\,\partial\omega} = \hbar \times b_{\text{coh}}^2 \sum_{\mathbf{q},s} \frac{k}{k_0} \times \delta(\hbar\omega \mp \hbar f) \times \frac{(2\pi)^3}{V} \times \frac{\hbar(n + \frac{1}{2} \pm \frac{1}{2})}{2Mf}$$
$$\times \sum_{m,n} \exp i(\mathbf{Q} \mp \mathbf{q}) \cdot (\mathbf{P}_m - \mathbf{P}_n] \times F_\tau^2 \times (\mathbf{Q} \cdot \mathbf{U})^2 \qquad (12)$$

where $\mathbf{P}_m$, $\mathbf{P}_n$ are lattice vectors which distinguish different unit cells and F is the unit cell structure factor[35].

Chain axis measurements for polyethylene and polytetrafluorethylene

The most widely used method of coherent INSS for observing phonons (quantized lattice vibrations) in perfect single crystals employs the 3-axis spectrometer developed by B. N. Brockhouse (see ref. 20). The instrument has two vertical axes to which are attached crystals for incident wavelength selection (I) and scattered neutron wavelength (hence energy) analysis (III) as well as one axis (II) for setting the orientation of the sample crystal to any angle with respect to the monochromatic beam produced by the first (wavelength selection) crystal and its subsequent collimator. Neutrons from the final analysing crystal are detected and counted as a function of the energy change on scattering very much as in Raman scattering experiments. A simplified description of the operation of this instrument has been given[18,43].

The 3-axis arrangement gives great flexibility in experiments and in particular allows selective excitation of longitudinal or transverse phonons along any crystallographic direction through the combined operation of the scalar product, $(\mathbf{Q} \cdot \mathbf{U})^2$ and the structure factor terms

$$\sum_{m,n} \exp i[\mathbf{Q} \pm \mathbf{q}] \cdot [\mathbf{P}_m - \mathbf{P}_n]$$

in the cross section formula. The latter indicates that scattering will only be strong near points $\mathbf{P}_m - \mathbf{P}_n$ in the lattice (i.e. near a Bragg peak) and the former shows that modes with their polarization vector $\mathbf{U}$ along the momentum transfer, $\mathbf{Q}$ will be the most intense. The disadvantage of the method for polymers arises because the small solid angles used to define the energy and momentum resolution of the machine for perfect single crystal studies lead to very small counting rates and counting rate to background ratios for large mosaic spread materials. The problem hardly arises when single crystals (e.g. of metals) are the sample since their scattering is sharply peaked in angular and energy distribution.

Naturally, therefore the first applications of coherent INSS to polymers studied polyethylene[26] and polytetrafluorethylene[27,28] where a high degree of c axis alignment was produced by drawing and rolling. Deuterated polyethylene was used for the first experiment since the coherent scattering in hydrogen polyethylene is masked by the high incoherent cross section of hydrogen. Fluorine and carbon nuclei are largely coherent scattering by contrast.

For deuterated polyethylene, Feldkamp, Venkataraman and King succeeded in observing phonons along the c axis using a 3-axis spectrometer. These belong to the longitudinal acoustic, ν_5, mode of the same symmetry as the 'accordion' mode seen by Raman spectra in shorter chains. The frequencies corresponding to wavelengths between *ca.* 3 Å (30 nM) and about 20 Å (200 nM) were measured and plotted as a function of the inverse wavelength (*Figure 10*) to give the dispersion curve (compare *Figure 6* and ref. 43). The dispersion curve fits an isolated chain, nearest neighbour force constant model quite well and the limiting slope at small reduced wavevectors (long wavelength vibrations) gives a Young's modulus of 329×10^{10}

dyne cm^{-2} at approximately 20°C. Presumably this material was a high density polyethylene but more data on its physical characteristics would be valuable. No attempt was made to measure phonons perpendicular to the chain because of the very poor orientation in these directions.

For polytetrafluorethylene, La Garde, Prask and Trevino[28] used a variant of the 3-axis technique where the neutron beam was chopped and energy analysis performed by time-of-flight measurements. Again the *c* axis (chain axis direction) was studied because a relatively high orientation could be produced by wrapping an extruded fibre around a steel frame. The sample had a 'rocking curve' of 9° full width at half maximum. Many phonons were observed in the first half of the Brillouin zone corresponding approximately to the carbon–carbon repeat distance. Again they fit well on to the dispersion curve predicted by using an isolated chain, sixteen parameter valence force field[28] with nine transferred and seven adjustable parameters. The weakness of interchain interaction is also apparent from the lack of space group splitting in the infra-red and Raman spectra.

This measurement gives a *c* axis modulus for the 15/7 helix at 25°C of 222×10^{10} dyne cm^{-2} which is rather larger than the x-ray [0015] planes and calculated moduli (156 and 163×10^{10} dyne cm^{-2} respectively). This particular disagreement is analogous to that in polyethylene.

Measurements of the modulus perpendicular to the chain for polycrystalline materials

Various combinations of rolling and drawing produce orientation of the *a* and *b* axes of polyethylene[29]. However, in these directions the best oriented specimens still have diffraction 'rocking curves' whose widths at half height are more than 15° and so present 3-axis neutron techniques are rather unsuitable for phonon measurements. Time-of-flight instruments, normally dedicated to incoherent scattering, have larger solid angles for incident and scattered neutrons and may be adapted advantageously to gain intensity in coherent scattering experiments from polymers[24]. Only a brief outline of this technique will be given to show how the method may be applied to polycrystalline samples by exploiting the, often great, anisotropy in crystalline axes.

The experiments were done using the cold neutron time-of-flight spectrometers[30,31] on the 4H5 and 6H holes of the DIDO reactor at the AERE, Harwell, UK. *Figure 7* shows a single chopper version of these instruments diagrammatically, along with the neutron energy distributions at various parts of the instrument. A full discussion of the techniques of time-of-flight spectrometry has been given by Brugger[32]. Briefly, in the present apparatus (4H5), thermal neutrons from the reactor core are moderated in a vessel containing liquid hydrogen. The neutrons emerging from this moderator have a Maxwell–Boltzmann distribution of velocities peaked around a temperature of about 30°K. Fast neutrons and gamma rays are removed by total internal reflection in the beryllium single crystal and by absorption in a bismuth single crystal. The beam then passes on to a rotating chopper with curved slots. At B, the high energy tail of the spectrum has been removed and in the chopper a narrow energy band is selected near the maximum of the distribution. For very high resolution work two choppers may be used or the

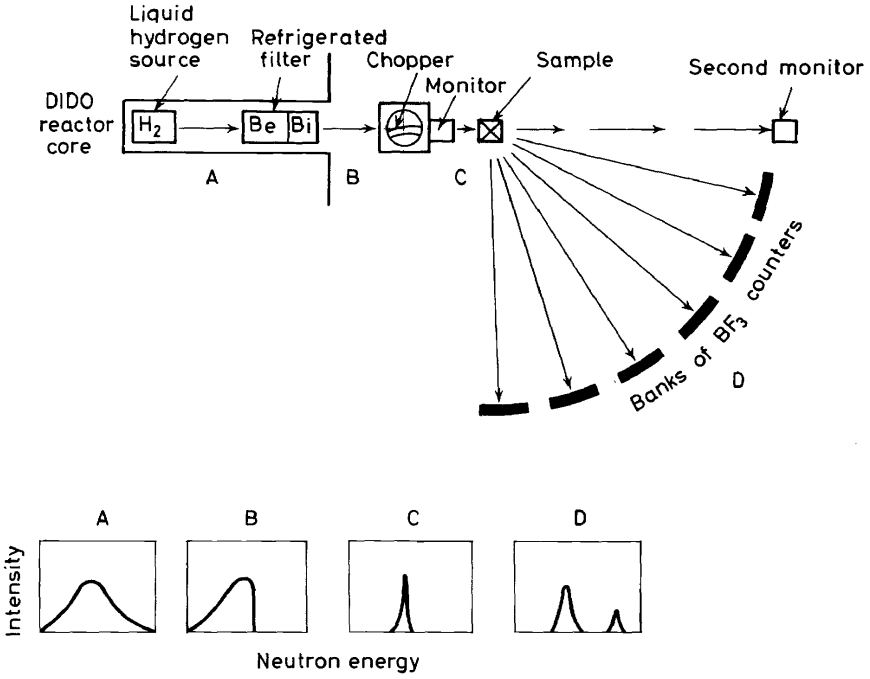

Figure 7. Chopper time-of-flight spectrometer for incoherent neutron scattering. For the experiments described the speed was adjusted so that 5.3 Å neutrons were passed by the chopper.

chopper passband may be set close to the beryllium total internal reflection cutoff wavelength. The rotating chopper not only selects a narrow band of energies but it also pulses the neutron beam. This pulsed beam is useful because the neutron energy for elastic and inelastic scattering may now be measured directly by the time-of-flight from sample to detectors. The intensity of the pulse incident upon the sample is measured by a monitor and after scattering the neutrons are collected over one quadrant in six banks of boron trifluoride counters.

Since the samples have been at room temperature, anti-Stokes scattering is the dominant inelastic effect. The number of neutrons as a function of their energy arriving at a given counter is shown in D in *Figure 7* and it can be seen that whilst most neutrons are scattered elastically a small group has gained a fixed amount of energy from quantized motions in the solid. Normally spectra are not presented with neutron intensity as a function of neutron energy but rather as the directly measured neutron intensity versus time-of-flight. In these time-of-flight spectra the energy gain peak is naturally on the LHS of the elastic peak. This will be so for the polyethylene spectra below.

The great gain in scattered intensity with this time-of-flight instrument comes from the large solid angle subtended by the collecting counters at the sample. The counters are at a given scattering angle, θ and are arranged

as closely as possible on a Debye–Sherrer circle with the beam as axis. Polycrystalline diffraction intensity is thus collected over an appreciable azimuthal angle.

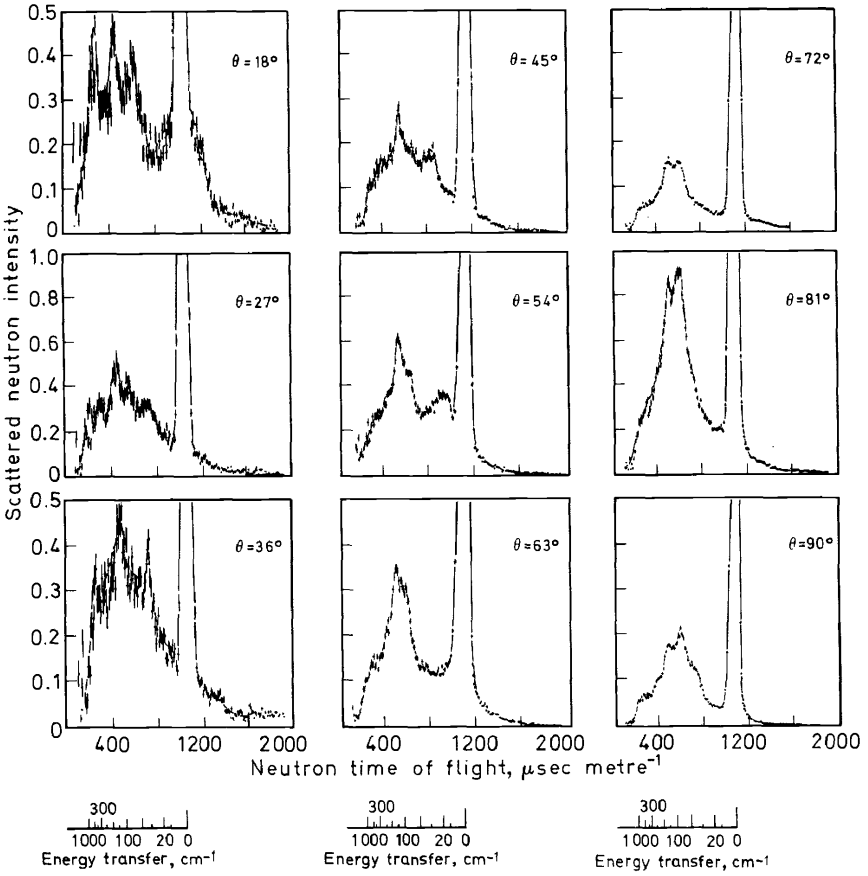

Figure 8. Neutron time-of-flight spectra for polycrystalline perdeuteropolyethylene, incident wavelength $\lambda = 4.2$ Å.

Figure 8 shows the neutron time-of-flight spectra from a high molecular weight, high density, polycrystalline sample of deuteropolyethylene. The sample had been studied extensively by x-ray[29] and neutron crystallography and was prepared by the method of Zeigler (see ref. 33).

The spectra were measured at nine angles of scattering to the incident beam and show a qualitatively different angular dependence from Raman scattering and incoherent neutron scattering spectra. One peak, in particular, can be seen to move to smaller energy transfers as the scattering angle increases. For $\theta = 18°$ the maximum is near 500 μs m^{-1}; at $\theta = 36°$ it is nearer 700 μs m^{-1}; at $\theta = 54°$ near 1000 μs m^{-1} and by $\theta = 63°$ it has merged with the elastic peak. By contrast other peaks associated with the

chain torsion etc. remain almost unchanged in frequency at different angles. From these much can be learned of the intramolecular force field but we concentrate on the 'moving' peak whose behaviour is characteristic of a phonon. We note that at about $\theta = 63°$ the elastic scattering intensity is greatly augmented by the presence of the intense 200 and 110 Bragg reflections of polyethylene.

The behaviour of this peak can be understood using the theory of polycrystalline and liquid scattering proposed by Cocking and Guner[34] and remembering the considerable anisotropy of the orthorhombic polyethylene crystalline unit cell ($a = 7.40$ Å, $b = 4.93$ Å, $c = 2.534$ Å). First we need the condition for elastic diffraction since intense coherent inelastic scattering occurs in conjunction with intense diffraction peaks.

A neutron beam of wavevector, $\mathbf{k}_0$, impinging on a rigid solid will be diffracted with momentum transfer $\mathbf{Q}$ if the vector condition (equation 13) is satisfied[35]

$$\mathbf{k} - \mathbf{k}_0 = \mathbf{Q} = 2\pi\boldsymbol{\tau} \tag{13}$$

where $\boldsymbol{\tau}$ is a reciprocal lattice vector and $\mathbf{k}$ is the outgoing wavevector of the neutron. In a normal 2θ scan this condition is fulfilled by various planes in turn as the scattering angle between $\mathbf{k}$ and $\mathbf{k}_0$, and hence $\mathbf{Q}$, increases. For a polycrystal this is also true except that all possible orientations of crystallites with respect to $\mathbf{Q}$ are possible and diffraction will occur when

$$|\mathbf{Q}| = 2\pi|\boldsymbol{\tau}| \tag{14}$$

The Debye–Sherrer ring pattern is produced. By working with cold neutrons (long wavelengths, small $\mathbf{k}_0$), $|\mathbf{Q}|$ can be kept within the first strong structure factor zone of an anisotropic crystal which means that diffraction may only occur from the most widely separated planes of those crystals properly oriented to the scattering plane of the apparatus. Since the static structure factor enters strongly into the inelastic scattering intensity (equations 11, 12) an extension of the same method to observe phonons along chosen crystal axes is possible. Clearly also the more crystallites have the correct orientation—the stronger are all effects. So by operating at low $\mathbf{Q}$ through the structure factor we have a method of choosing the crystalline axis to which neutron excitation of phonons will be referred.

We must now control whether the excited phonon is of longitudinal or transverse polarization. *Figure 9* shows the vectorial condition for coherent inelastic scattering. The diagram must satisfy the joint constraints of diffraction and energy transfer, namely

$$\begin{aligned}\mathbf{k} - \mathbf{k}_0 = \mathbf{Q} &= 2\pi\boldsymbol{\tau} \pm \mathbf{q} \\ &= \mathbf{Q}_{\text{lattice}} \pm \mathbf{q}_{\text{phonon}}\end{aligned} \tag{15}$$

and

$$(\hbar/2m)(k^2 - k_0^2) = \hbar\omega_{\text{phonon}} \tag{16}$$

where m is the neutron mass, $\hbar\omega_{\text{phonon}}$ the energy of the excited phonon and $\mathbf{Q}_{\text{lattice}}$ refers to that part of the momentum transfer associated with elastic scattering only.

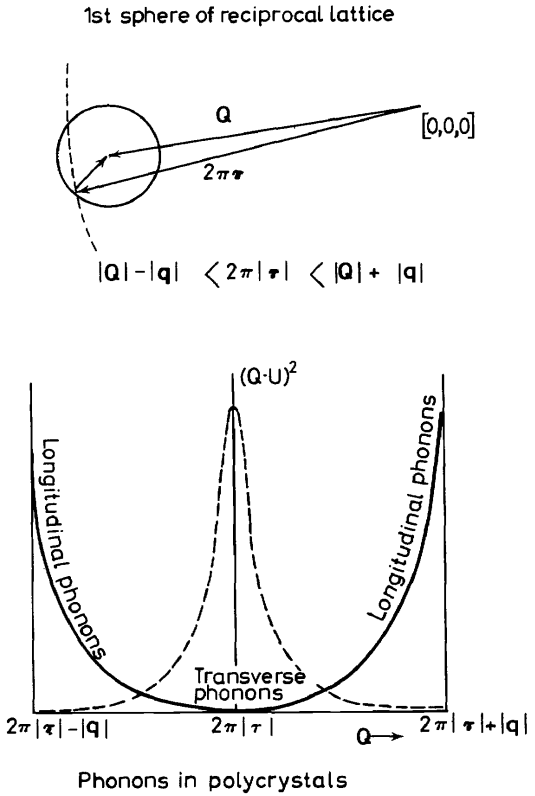

Figure 9. Vector diagram and theoretical spectrum for phonons in an anisotropic polycrystal [After Twisleton and White[24]].

If $\mathbf{q}$ is the wavevector of the phonon, $\mathbf{Q}$, $\mathbf{q}$ and $2\pi\tau$ make up a triangle and the permissible range of $\mathbf{q}$ is

$$|\mathbf{Q}| - |\mathbf{q}| < 2\pi|\tau| < |\mathbf{Q}| + |\mathbf{q}| \tag{17}$$

All phonons in this range will be observed. The broad band which moves through the diagrams of *Figure 8* is composed of many phonons of intermediate polarization vectors. Of this group *Figure 9* shows that three unique points may be identified. At $|\mathbf{Q}| = 2\pi|\tau| \pm |\mathbf{q}|$, i.e. with $\mathbf{Q}$, $2\pi\tau$ and $\mathbf{q}$ collinear there are two cutoff points. These have great intensity and unique longitudinal polarization because of the scalar product $|\mathbf{Q} \cdot \mathbf{U}|^2$ in the cross section formula. Furthermore because diffraction is simultaneously necessary for the inelastic scattering we can be sure that the phonons are excited in microcrystalline regions. There is also the diffraction maximum at $2\pi|\tau| = |\mathbf{Q}|$ where transverse phonons are excited and which corresponds to a crystalline lattice plane spacing.

In our experiments (*Figure 8*) only the $2\pi|\tau| - |\mathbf{q}|$ cutoff is observed for experimental reasons. This can be taken as the maximum of intensity in our spectra and since both its frequency, ω, and wavevector, $\mathbf{q}$, are determined we can plot the dispersion curve. In deuteropolyethylene the *a* crystallo-

graphic direction is longest and the observed phonon in *Figure 8* is most probably the longitudinal acoustic oscillation in this direction perpendicular to the chains. The only ambiguity comes from the nearby [110] peak in the structure factor, which may allow [110] phonons to be excited.

Figure 10 shows the *a* axis and *c* axis dispersion curves plotted as a function of reduced wavevector (e.g. $2\pi/a = 1$). The great difference in slope near the Brillouin zone centre is obvious and leads to sound velocities of 1.715×10^6 cm sec^{-1} and 1.35×10^5 cm sec^{-1} for the two directions. Using a density of $\rho = 1.149$ g cm^{-3} from the crystal structure the moduli are $E_c = 329 \times 10^{10}$ dyne cm^{-2}, and $E_a = 6 \times 10^{10}$ dyne cm^{-2}. The curve for the phonon is almost straight within the zone defined by $-\pi/a < \mathbf{q} < \pi/a$, a possible consequence of the almost hexagonal symmetry of this crystal. The consequences for the modulus of the great temperature sensitivity of this direction are being investigated. The formal assignment of the phonon, above, to the *a* direction rather than [110] may be revised by current high resolution studies combined with dynamical structure factor analysis.

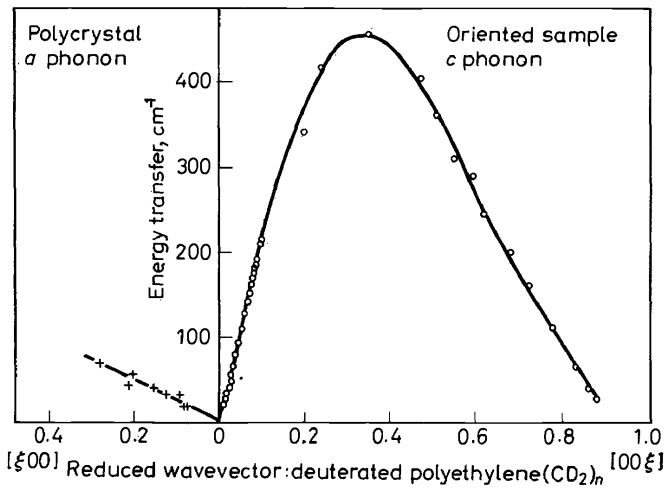

Figure 10. Dispersion curves for deuteropolyethylene along the *a* and *c* crystallographic directions [After Twisleton and White[24]].

Relation between $E_{\text{stat.}}$ and $E_{\text{dyn.}}$

The results above have shown that modulus measurements with spectroscopy generally give larger values than x-ray, sound wave or static tests and it is a fair question to ask if these higher values are indeed the true values to be aimed at or whether there is some systematic bias in the techniques.

The higher values suggest a correlation with past experience that high frequency dynamic methods usually give higher moduli than static tests due to relaxation phenomena in the polymer.

First it must be made clear that the spectroscopic measurements are confined, at present, to the microcystalline, crystalline regions and that the effects of crystallite texture will be to produce boundary condition effects

on such quantities as phonon lifetime. Under these conditions a case can be made for the correspondence of spectroscopic and static measurements.

In an extended isolated simple chain such as a planar zig-zag, to which we have seen the segments in polyethylene crystallites correspond quite well, we might expect no dispersion of the sound velocity until the sound wavelengths approached the interatomic separations. Putting this slightly differently, the chain should behave as a harmonic oscillator up to a harmonic number corresponding to these short wavelengths. This means that over the full range of atomic displacements produced by the harmonics, the potential energy will be quadratic in the displacement and the wave frequency and wavelength inversely proportional through the sound velocity. That Hooke's law is so obeyed from the bottom of the potential well of the configuration coordinate (accordion mode stretch) of alkanes can be seen from *Figure 6* where for a large number of harmonics the simple relation is true.

In a static measurement the same configurational coordinate is changed and the potential energy of the chain 'moves up' the same quadratic curve that is explored by the vibrational spectrum. For such a situation Young's modulus will be independent of the method.

For more complicated chain conformations or in a chain with side groups additional dispersions in the sound velocity are to be expected. Here also the caveat[6] about type of sound propagation must be mentioned. This proviso may also be important in some specimens of polyethylene for directions perpendicular to the chain axis since phonons are not being excited in a crystal of infinite extent. For our sample the mosaic blocks were large enough not to damp out phonons whose wavelength was less than about 20 Å.

3. EXPERIMENTAL VALUES FOR ELASTIC MODULUS ALONG THE CHAIN—$E_{\parallel}$

When a crystalline polymer like high density polyethylene or nylon is oriented by drawing, the overall modulus in the draw direction increases markedly. With a highly oriented specimen, the molecular arrangement can be regarded to a first approximation as a series arrangement of crystalline and amorphous regions (*Figure 11*; see for example also ref. 7), and if the moduli are represented as E_0, $E_{\parallel}$ and E_a, for the overall oriented specimen in the draw direction, the crystalline regions and the amorphous regions respectively, then

$$(1/E_0) = (1 - V_c)/E_a + V_c/E_{\parallel} \tag{18}$$

where V_c is the volume fraction of the crystalline phase. A minor problem in using this equation is that E_a, the modulus of the amorphous region cannot be regarded as invariant since the amorphous phase may itself be oriented to a greater or lesser extent by the drawing operation. For example Dulmage and Contois[12] found that E_a could be increased by a factor of three by drawing.

The overriding influence of the amorphous region in a series arrangement can be illustrated by the following imaginary case. Suppose $V_c = 0.5$, $E_a = 2 \times 10^{10}$ dyne cm^{-2} and $E_{\parallel} = 200 \times 10^{10}$ dyne cm^{-2}. These data

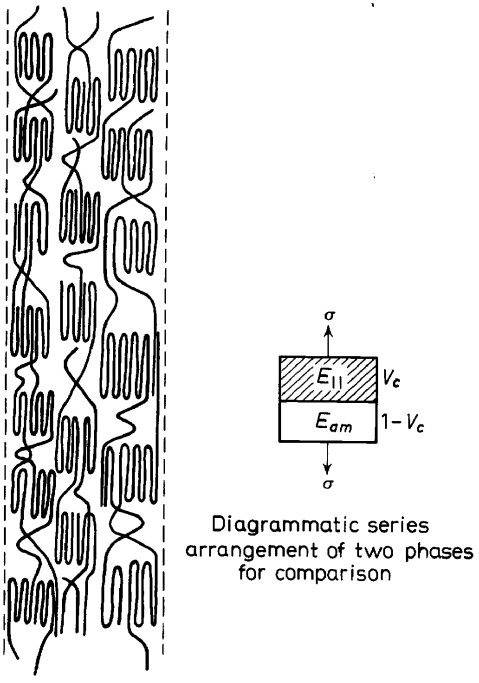

Figure 11. Diagrammatic arrangement of crystalline and amorphous regions in an oriented polymer fibre.

are not too far from the case of polyethylene, E_a being higher than the isotropic amorphous material because of the effect of orientation.

$$\frac{1}{E_0} = \frac{0.5}{2 \times 10^{-10}} + \frac{0.5}{200 \times 10^{-10}} \text{ cm}^2 \text{ dyne}^{-1} \tag{19}$$

$$E_0 = 4 \times 10^{10} \text{ dyne cm}^{-2}$$

Whilst examining the data in *Table 1*, it should be borne in mind that the overall modulus E_0 of fibres in practice is of the order of 2–10 $\times$ 10^{10} dyne cm^{-2}. The results of this work are shown on the LHS of *Table 1*, which shows the measured moduli in the chain direction of the crystalline regions of a number of polymers. In the great majority of cases, the x-ray method was used. This is the most direct method, since a stress is applied to the specimen and the resulting extension is measured. It suffers from the drawback, already mentioned, that it is assumed that the overall applied stress is identical with the stress which is transferred to the crystalline regions. In two cases, low-frequency Raman scattering spectra were used to calculate the modulus. There is one example of INSS applied to deuterated high density polyethylene from which the longitudinal modulus has been calculated. In any discussion on the stiffness of polymers, a case can be made for including the Raman and neutron spectroscopy values in either the measured or the theoretically

calculated series of figures. We have chosen to class them as measured values.

The experimental results set out on the LHS of *Table 1* are also shown graphically in *Figure 12* for convenience. It will be seen that the measured elastic modulus parallel to the chain axis varies from about 358×10^{10} dyne cm^{-2} for polyethylene (to take the highest value) to 4.1×10^{10} dyne cm^{-2} for polyvinyl tert butyl ether—a factor of nearly *ninety* times. In contrast, as will be seen later, the elastic moduli perpendicular to the chain will be in the region of about 3×10^{10} dyne cm^{-2}, with a range of only about *three* times.

The data in *Table 1* show that, apart from diamond and graphite (parallel to the layer planes), the highest moduli are encountered with the planar zig-zag conformation. The examples in question are polyethylene and polyvinyl alcohol. It will be seen that there is a marked drop in going even to the very lazy helix (15/7) of polytetrafluorethylene which departs only slightly from the planar zig-zag. This point is well brought out in the pioneering paper of Dulmage and Contois[12]. They investigated the elastic modulus and extensivity of the crystalline regions of a range of highly oriented fibres. The eight polymers were polyesters or polyesteramindes, one of which was polyethylene terephthalate. A low modulus could be associated unequivocally with a contracted fibre identity period (FIP) as the following data, taken from their work, show:

	Contraction of fibre identity period	$E_{\parallel}$ for crystalline regions, dyne cm^{-2}
Mean of two fully extended polymers	$\sim 0\%$	135×10^{10}
Mean of six contracted examples	20%	5×10^{10}

As these authors pointed out, 'whenever very high elastic modulus is important, the polymers with contracted FIPs are probably basically deficient', In the case of polyethylene, it is possible to compare directly results based on x-ray measurements with those based on Raman and neutron spectra. The x-ray results are much lower—240×10^{10} compared with 340×10^{10} dyne cm^{-2}—which leads one to query, as one possible reason for the discrepancy, the assumption of uniform stress. If the modulus $E_{\parallel}$ of polyethylene in the crystalline regions is more correctly represented by the value 340×10^{10} dyne cm^{-2}, the conclusion might be drawn that the local stress in these regions is higher than the average stress. A ratio of $\sigma_{local} : \sigma_{average}$ of $340/240 = 1.4$ would be needed to account for the strains observed. On the other hand, the work of Sakurada *et al.* referred to above (refs. 10, 14) tends to support the assumption of homogeneous stress. As already discussed, this difference cannot be explained in terms of dynamic versus static measurements. It therefore remains unresolved at this stage.

There is a considerable discrepancy between the two results for polyethylene terephthalate, obtained independently by Dulmage and Contois[12] and by Sakurada, Ito and Nakamae[10], these being 140 and 76×10^{10} dyne cm^{-2} respectively. It is suggestive that the former is closer to the theoretical figure, but otherwise it is impossible to account for the difference.

Before turning to the theoretical calculations of $E_{\parallel}$, it is interesting to compare these values for stiffness, and specific stiffness, with other materials.

P.A.C.—26/3-4K

Table 1. Experimental and calculated value

$E_{\parallel}$ measured

Ref.	*Polymer*	*Method*‡	*Value*§ *of* $E_{\parallel}$ dyne cm^{-2}	*Comments*	*Date*	*Authors*
10	Cellulose I	x-ray*	130×10^{10}	Staggered ring	1964	Sakurada, Ito and Nakamae
10	Cellulose II	x-ray	90×10^{10}	Staggered ring	1964	Sakurada, Ito and Nakamae
10	Polyethylene	x-ray	240×10^{10}	Planar zig-zag	1964	Sakurada, Ito and Nakamae
41		Raman	340×10^{10}		1949	Mizushima and Shimanochi
42		Raman	358×10^{10}		1967	Shauffele and Shimanouchi
26		neutron	329×10^{10}	$(CD_2)_n$	1968	Feldkamp, Venkataraman and King
10	Polypropylene (isotactic)	x-ray	42×10^{10}	3/1 helix	1964	Sakurada, Ito and Nakamae
10	Polyoxymethylene	x-ray	54×10^{10}	9/5 helix	1964	Sakurada, Ito and Nakamae
10	Polytetrafluor-ethylene	x-ray	156×10^{10}	15/7 helix	1964	
12	Poly(ethylene-terephthalate)	x-ray	140×10^{10}	planar zig-zag	1958	Dulmage and Contois†
10		x-ray	76×10^{10}		1964	Sakurada, Ito and Nakamae
10	Polyvinyl alcohol	x-ray	255×10^{10}	Planar zig-zag	1964	Sakurada, Ito Nakamae
10	Polystyrene	x-ray	12×10^{10}	Helix	1964	Sakurada, Ito and Nakamae
10	Nylon 6	x-ray	25×10^{10} α Form 21×10^{10} γ Form	Planar zig-zag	1964	Sakurada, Ito and Nakamae
	Nylon 66					
10	Polyethylene oxide	x-ray	10×10^{10}	Helix	1964	Sakurada, Ito and Nakamae
	Polyvinyl chloride			Helix		

for elastic moduli along the chain —$E_{\parallel}$

$E_{\parallel}$ calculated

Ref.	*Method*	*Value of* $E_{\parallel}$ dyne cm^{-2}	*Comments*	*Date*	*Authors*
36	2 constant valence force field	77 or 121 × 10^{10}		1936	Meyer and Lotmar
37	2 constant valence force field	180 × 10^{10}		1958	Lyons
38	2 constant valence force field	56 × 10^{10}		1960	Treloar
38	2 constant valence force field	182 × 10^{10}		1960	Treloar
44	4 constant Urey–Bradley force field	340 × 10^{10}		1962	Shimanouchi, Asahina and Enomoto
46	8 constant Urey–Bradley force field	256 × 10^{10}		1966	Odajima and Maeda
45	4 constant Urey–Bradley force field	49 × 10^{10}		1962	Asahina and Enomoto
45	4 constant Urey–Bradley force field	(220 or) 150 × 10^{10}		1962	Asahina and Enomoto
44	4 constant Urey-Bradley force field	160 × 10^{10}		1962	Shimanouchi, Asahina and Enomoto
37	2 constant valence force field	146 × 10^{10}		1958	Lyons
38	2 constant valance force field	121 × 10^{10}		1960	Treloar
37	2 constant valence force field	157 × 10^{10}		1958	Lyons
38	2 constant valence force field	196 × 10^{10}		1960	Treloar
55	4 constant Urey–Bradley force field	13 × 10^{10}	compare value in ref. 24	1969	Matsuura and Miyazawa
45	4 constant Urey–Bradley force field	200, 230, 160 × 10^{10}	syndiotactic	1962	Asahina and Enomoto

P.A.C.—26/3—4K*

Table 1

$E_{\parallel}$ measured

Ref.	*Polymer*	*Method*‡	*Value*§ *of* $E_{\parallel}$ dyne cm^{-2}	*Comments*	*Date*	*Authors*
	Polyisobutylene			Helix		
10	Polybutene I (form I)	x-ray	25×10^{10}	Helix	1964	Sakurada, Ito and Nakamae
10	Polyvinyl tert butyl ether	x-ray	4.1×10^{10}	Helix	1964	Sakurada, Ito and Nakamae
10	Polytetrahydro-furan	x-ray	55×10^{10}	Planar zig-zag	1964	Sakurada, Ito and Nakamae
10	Polyvinylidene chloride	x-ray	41.5×10^{10}	?	1964	Sakurada, Ito and Nakamae
	Poly-3,3-bis-halo-methyl oxycyclo-butanes			Planar zig-zag		
54	Diamond		800×10^{10}			
54	Graphite		450×10^{10} 1000×10^{10}	Carbon fibre Graphite (basal plane)		

* For further information on the lattice planes used for measurements, see refs. 10 and 12.

† This important paper contains modulus data on seven other condensation polymers, with $E_{\parallel}$ ranging from 3.7 to 130 $\times 10^{10}$ dyne cm^{-2}.

The high specific stiffness of the polyethylene crystal, in the chain direction, is noteworthy, see *Table 2.*

Table 2. Young's modulus, and specific modulus, of a range of materials

	Specific gravity ρ	Modulus, E (10^{10} dyne cm^{-2})	E/ρ (10^{10} dyne cm^{-2})
Aluminium	2.7	71	26
Iron	7.8	205	26
Glass	2.5	68	27
Beryllium	1.8	302	168
Silicon carbide	3.2	547	171
Carbon	2.3	1000	439
High density polyethylene (isotropic)	0.95	1.4	1.4
High density polyethylene (fibre)	0.95	15	15
High density polyethylene (crystal-$E_{\parallel}$)	1.00	350	350

4. THEORETICAL VALUES FOR ELASTIC MODULI ALONG THE CHAIN $E_{\parallel}$

The pioneering theoretical work of estimating the modulus of elasticity of polymers was carried out by Meyer and Lotmar[36]. They showed in 1936 that the modulus corresponding to the principal chain direction of a polymer

continued

		$E_{\parallel}$ calculated			
Ref.	*Method*	*Value of* $E_{\parallel}$ dyne cm^{-2}	*Comments*	*Date*	*Authors*
45	4 constant Urey–Bradley force field	8.4, 7 × 10^{10}		1962	Asahina and Enomoto
45	4 constant Urey–Bradley force field	77–110 × 10^{10}	(passing from iodine to fluorine as halogen)	1962	Asahina and Enomotc

‡ The temperature at which the modulus was measured in the various experiments falls within the range 20° to 28°C. See refs. 10 and 12.
§ The specimen moduli (as opposed to the modulus $E_{\parallel}$ of the chain in the crystalline region) fall within the range 2 to 23 × 10^{10} dyne cm^{-2}. See refs. 10 and 12.

crystal could be calculated from the force constants of the chemical bonds of the chain derived from vibration frequencies of other molecules. They applied this method to cellulose, considering two modes of deformation—bond stretching and bond angle opening. The method was extended by Lyons[37] to nylon 66 and polyethylene terephthalate, and by Treloar[38] to polyethylene. Treloar also re-examined the work of Meyer and Lotmar, and Lyons, and his calculations represent the latest refinement of the valence force field 2 constant type.

The nature of this method will now be explained. Only the chain atoms are considered, and the effect of interchain forces is neglected. In the case of a planar zig-zag molecule like polyethylene, consider a force F acting along the chain. If θ is the angle of inclination of each carbon–carbon bond to the

Polyethylene chain

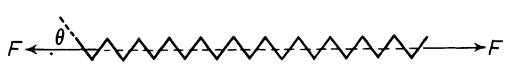

chain axis, then the change of length δl caused by the application of force F is (ref. 17)

$$\delta l = nF[\cos^2\theta/k_1 + \sin^2\theta/4k_p] \tag{20}$$

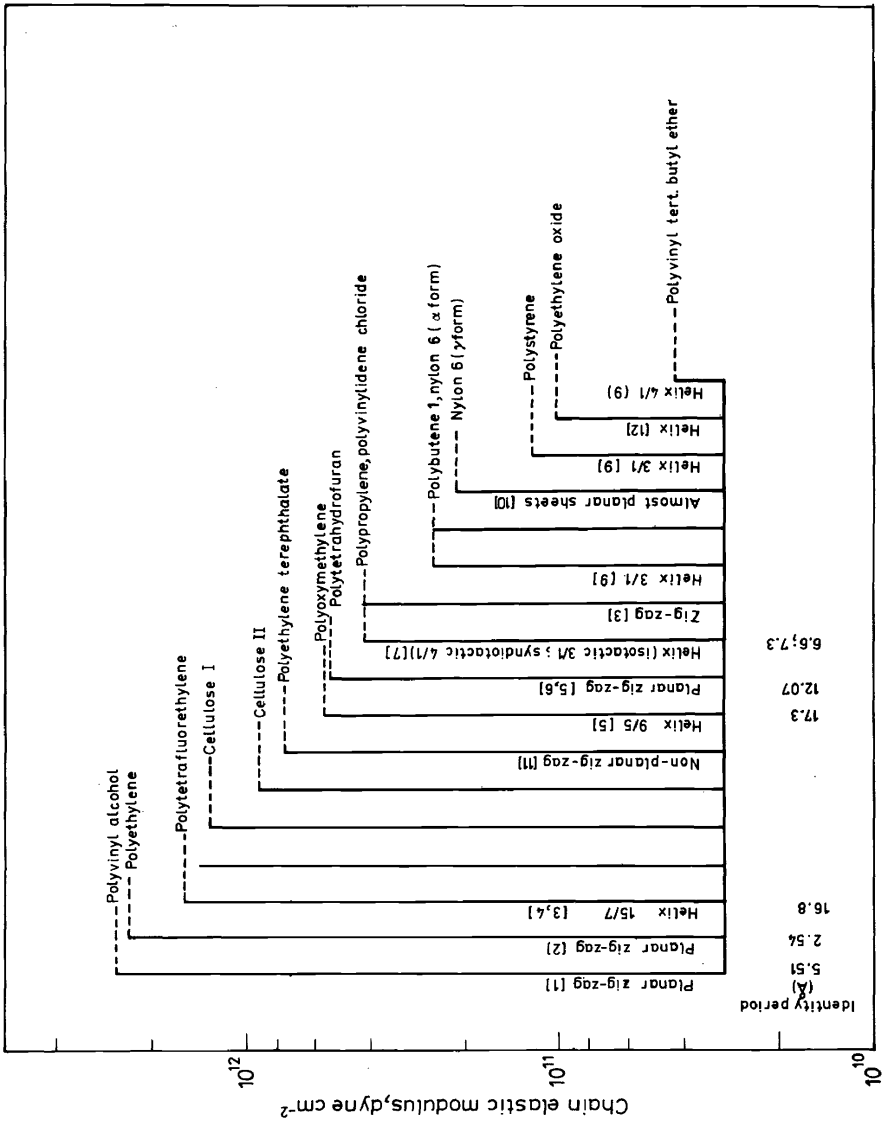

Figure 12. Range of measured polymer elastic moduli in the chain direction.

where n is the number of bonds, k_1 is the force constant for bond stretching, and k_p is the force constant for valence angle opening (for the definition of k_1 and k_p, see ref. 17). Using the formula

$$E = (F/A)/(\delta L/L) \tag{21}$$

and knowing the cross-sectional area of the chain A, the elastic modulus can be calculated. The force constants used by Meyer and Lotmar, Lyons and Treloar are shown in *Table 3*.

From this, the care taken by Treloar to choose the most suitable force constants is evident. Nevertheless, the method cannot be regarded as being very unrefined in comparison with more recent work, and it tends to give low values when compared with experiment.

In connection with this valence force field type of calculation, the simple approach of Dulmage and Contois based on force constants similar to *Table 3* is of considerable interest[12]. The results of their calculations are shown in *Figure 13* and *Table 4*. They considered extension in the chain

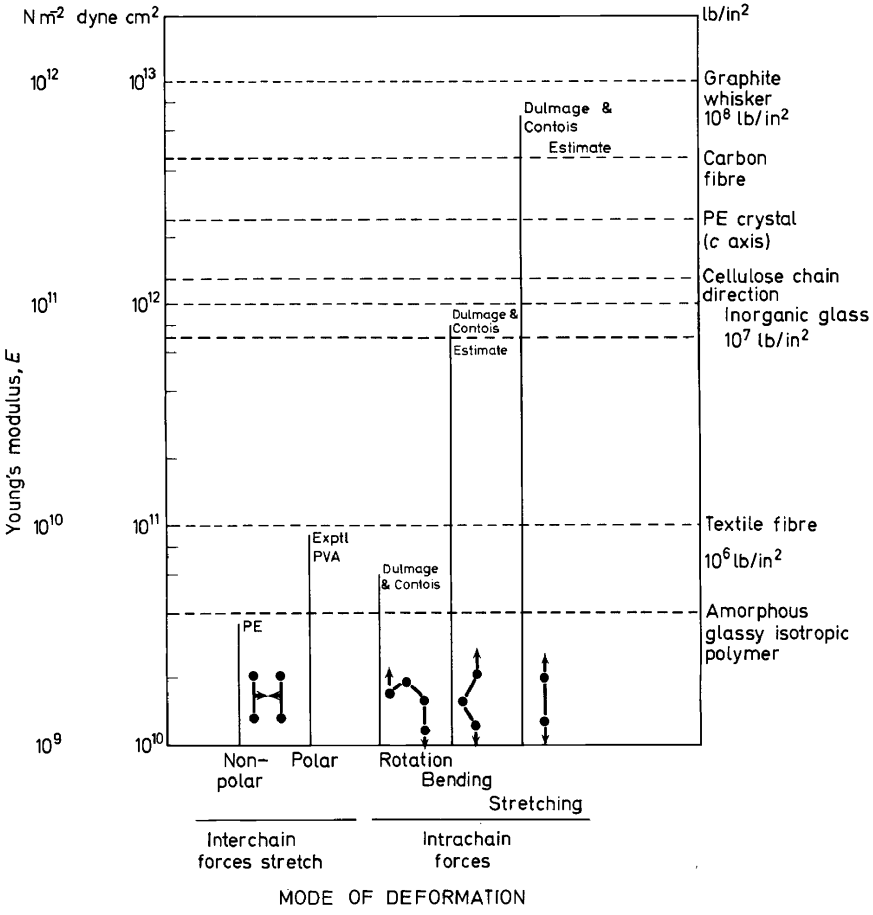

Figure 13. Moduli based on fundamental deformation mechanisms.

Table 3. Constants used in valence field calculations of $E_{\parallel}$

	Meyer and Lotmar 1936	Lyons 1958	Treloar 1960
		Stretching constants k_1 (dyne cm^{-1})	
C—C	4.3×10^5	5.0×10^5 (paraffin)	4.36×10^5 (paraffin—planar)
			4.52×10^5 (paraffin—pyramidal)
		7.6×10^5 (aromatic)	7.62×10^5 (aromatic)
C—O	5.0×10^5	5.4×10^5	4.54×10^5
C—N	—	5.3×10^5	7.8×10^5 (OC—NH)
			5.74×10^5 (H_2C—NH)
		Bending constants k_p (dyne cm^{-1})	
	Considered $k_p = \frac{k_1}{k_{10}}$	Assumed $k_p = \frac{k_1}{5}$	C—C—C 0.35×10^5 (paraffin—planar)
			C—C—C 0.4×10^5 (paraffin—pyramidal)
	also $k_p = \frac{k_1}{5}$	based on Bartholomé and Teller[39]	C—C—C 0.66×10^5 (aromatic)
	based on a generalization of Bartholomé and Teller		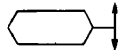 1.06×10^5
			C—C—N 0.365×10^5
			C—C(O)—N 0.38×10^5
			C—C—O 0.52×10^5
			C—O—C 0.43×10^5
			C—N—C 0.68×10^5

direction, according to three quite distinct modes. The stiffest mode is represented by the extension of a single bond, next came valence angle opening, the third being rotation around bonds. The resistance to deformation in these three cases is roughly in the ratio of 100:10:1.

Table 4. Moduli along the chain ($E_{\parallel}$) based on alternative modes of deformation

	Equivalent modulus dyne cm^{-2}	Source
Bond stretching	740×10^{10}	Dulmage and Contois[12]
Valence angle opening	80×10^{10}	Dulmage and Contois[12]
Bond rotation	6×10^{10}	Dulmage and Contois[12]
Bond rotation	6×10^{10}	P. B. Bowden[40]

At the moment there is no known carbon polymer with a modulus controlled solely by bond stretching. In the experimentally realizable type of stiff chain such as polyethylene, valence bond opening plays a very important role. However, the mechanism of bond rotation can be seen to be controlling in many cases, as is evident on comparing *Figure 12* with *Figure 13*, and as showed up quite clearly in Dulmage and Contois's own modulus measurements discussed earlier. They concluded that the higher modulus polymers extended by the bond stretching, and bond angle opening mechanisms, but for the lower modulus materials, the fundamentally different mechanism of simultaneous internal rotation of all chains in the crystalline region would be the controlling process. This would also correlate with a contracted fibre identity period.

The first improvement of the valence force field type of calculation, in an attempt to simulate the elastic modulus determined from Raman scattering measurements, introduced a Urey–Bradley force field for the molecule. Shimanouchi, Asahina and Enomoto[44] included contributions from interatomic repulsions and bond twisting as well as the carbon–carbon stretch and bending modes of deformation in their expression for the potential energy of the polyethylene molecule. For this calculation the CH_2 groups were treated as a single dynamical unit thus avoiding the need for the H—H force constants. The extra force constants required for this calculation were obtained from Raman data for paraffin hydrocarbons[41] and the value obtained for the elastic modulus of the chain was 340×10^{10} dyne cm^{-2}, in complete agreement with the earlier Raman measurements. A tantalizing situation then arose, when the theoretical calculation gave a higher value for $E_{\parallel}$ than the x-ray measurements of Sakurada, Ito and Nakamae. Asahina and Enomoto went on[45] to calculate the modulus of a number of other polymer chains. In the case of certain helical arrangements such as polyethylene oxide and polyisobutylene, they predicted values of $E_{\parallel}$ in the neighbourhood of 4–8 $\times 10^{10}$ dyne cm^{-2} which agreed well with subsequent x-ray measurements as shown in *Table 1*. A later calculated value for polyethylene oxide[51] gave a modulus of 13×10^{10} dyne cm^{-2}.

The most recent refinement in the theoretical calculation of the chain axis modulus of polyethylene comes from Odajima and Maeda[46] in 1966. A Urey–Bradley force field was used for the intramolecular interactions, but instead of the carbon skeleton model as used previously[44], stretching constants were used for, C—C, C—H; angle bending constants for C—C—C, H—C—H, C—C—H and non-bonding constants for carbon–carbon, hydrogen–hydrogen and carbon–hydrogen interactions within the chain. The constants used were taken from the data of Shimanouchi *et al.*[47], and Schachtschneider and Snyder[48]. In addition, the intramolecular force field was considered, and interaction potentials of the 6-exponential, and Lennard-Jones 6-12 types were both used. This calculation attempts the ultimate sophistication in molecular crystal static calculations. Values of the long axis and various transverse moduli were obtained (with the latter of which we deal later). The *c*-axis modulus was calculated to be 256×10^{10} dyne cm^{-2}, and how this compares with other calculations, and with the experimental data, can be seen from *Table 1*. It is of the same order as the x-ray measurement, but considerably lower than the moduli determined from Raman and neutron data. It is interesting to note that the contribution to E_c from the intramolecular part of the interaction was found to be only 0.2 per cent. It is unlikely that the discrepancy between the calculations of Odajima and Maeda, and the Raman and neutron scattering values can be explained by the intermolecular constants chosen, since the axial modulus is so insensitive to the transverse force field.

5. EXPERIMENTAL VALUES FOR ELASTIC MODULUS TRANSVERSE TO THE CHAIN $E_\perp$

In comparison with experimental and theoretical work dealing with the longitudinal modulus, relatively little has been done in the transverse direction. A summary of this work is shown in *Table 5*. The general picture which emerges is consistent with our understanding of intermolecular forces—the moduli are much lower than in the chain direction, and the range covered varies by a factor of only three. Furthermore, the x-ray measurements appear to be self-consistent as we seek to show in *Figure 14*.

In this, the average values of the transverse moduli are plotted against the cohesive energy density of the material. It would be expected that the more polar the polymer—this criterion being measured adequately by cohesive energy density—the higher the transverse modulus. This hypothesis seems to be borne out adequately by *Figure 14*.

Against this must be set the rather higher value for E_a obtained by the Odajima and Maeda calculation and by Twisleton and White[24] using neutron spectroscopy. Their figure of 6.0×10^{10} dyne cm^{-2} should be compared with the mean x-ray figure for E_a of polyethylene of 3.3×10^{10} dyne cm^{-2}. As pointed out above, in the discussion on experimental methods, it does not appear that this discrepancy can be explained by reference to the fact that one is a dynamic, the other a static measurement. Furthermore, the Samuels value of 4.0×10^{10} dyne cm^{-2} obtained by using sound wave measurements is of the same order as the x-ray figure. We must leave the

subject in this unsatisfactory state until further experimental work clarifies these differences.

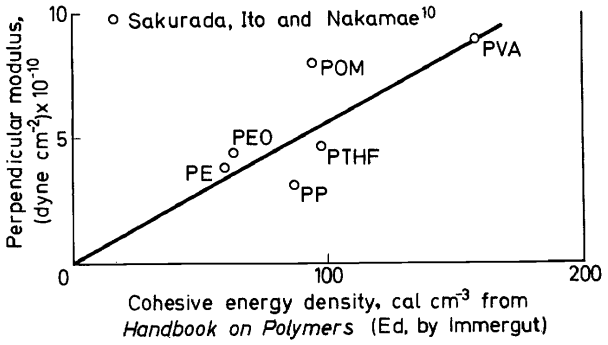

Figure 14. Plot of moduli perpendicular to chain against cohesive energy density.

6. THEORETICAL VALUES FOR ELASTIC MODULUS TRANSVERSE TO THE CHAIN $E_\perp$

Table 5 also shows the calculated values for $E_\perp$, which can be compared with the measured values. Apart from a figure for graphite at right angles to the layer planes, and a calculated figure for argon, these values all pertain to polyethylene. It will be seen that there are considerable differences in them.

The work was pioneered by Enomoto and Asahina[49], and Miyazawa and Kitagawa[50], who both used a carbon skeleton, nearest neighbour only force field for the lattice modes of the polyethylene crystal. Hydrogen interactions included in the lattice force field were derived by using intermolecular potential data for methane. Quite different sets of results were obtained by these authors, the first giving $E_a = E_b = 2.1 \times 10^{10}$ dyne cm^{-2}, whilst the latter authors' calculation gave $E_a = 5.7 \times 10^{10}$ dyne cm^{-2} and $E_b = 2.1 \times 10^{10}$ dyne cm^{-2}. There is an even greater difference in the values attributed to Miyazawa and Kitagawa by Sakurada[10], where $E_a = 6.7 \times 10^{10}$ and $E_b = 10.8 \times 10^{10}$ dyne cm^{-2}. Both calculations paralleled the Shimanouchi Urey–Bradley field for the intramolecular motion, and used three external force constants only between atoms in the crystal unit cell. This procedure seemed justified by work on the external vibrations of *n*-paraffins, whose intermolecular forces have been shown to be mainly of the van der Waals type[51]. The Miyazawa and Kitagawa calculation[50] of the density of crystal phonon states agrees quite well with incoherent, inelastic neutron scattering measurements[22,43] and it agrees with low temperature specific heat measurements for the polyethylene crystal.

Finally the extended calculations of Odajima and Maeda[46] also treated exhaustively the lattice moduli in the transverse direction. Two sets of values which differed only slightly were obtained, depending on the interatomic constants chosen. These support the possibility that $E_b > E_a$ and suggest a higher value for E_a than the x-ray data.

Table 5. Experimental and calculated values for elastic moduli transverse to the chain—$E_\perp$

Polymer	$E_\perp$ measured Modulus normal to lattice planes $E \times 10^{-10}$ dyne cm^{-2} 110	200 (E_a)	020(E_b)	Other	Method	Authors (ref.)
Polyethylene	4.3	3.2	3.9	—	x-ray	Sakurada, Ito and Nakamae (10)
	—	3.2	3.9	—	x-ray	Quoted by Odajima and Maeda (46)
		2.5 5.0	1.9			
	6.0*	6.0*	—	—	neutron	Twisleton and White (20)
Polypropylene		2.9		3.2(040)	x-ray	Sakurada, Ito and Nakamae (10)
				4.0	sonic	Samuels (8)
Polyvinyl alcohol		8·9		9.0 (10$\bar{1}$)	x-ray x-ray	Sakurada, Ito and Nakamae (10)
				4.7 (002)		
Polyoxymethylene				8.0 (10$\bar{1}$0)	x-ray	Sakurada, Ito and Nakamae (10)
Polytetrahydrofuran		4.6	4.6		x-ray	Sakurada, Ito and Nakamae (10)
Polyethylene oxide				4.4 (120)	x-ray	
Graphite ⊥ to layer planes				39	neutron	
Hexadecane crystal	1.5				neutron	Twisleton
Argon				3.0	sonic	

Polymer	$E_\perp$ calculated Modulus $E \times 10^{-10}$ dyne cm^{-2} 110	200 (E_a)	020 (E_b)	Comments	Authors (ref.)	
Polyethylene		5.7	2.1	Urey–Bradley molecular field Lennard–Jones intermolecular	Miyazawa and Kitagawa (50)	
		6.7	10.8	Quoted by Sakurada, Ito and Nakamae (10)	Miyazawa and Kitagawa	
		2.1	2.1		Enomoto and Asahina (49)	
	4.91	4.76	8.33	6 exponential potential with two sets of interatomic constants	Odajima and Maeda (46)	Set I
	6.84					Set III

* The same number is quoted for each direction here in view of the ambiguity mentioned on page 562.

7. THE PROBLEM OF ISOTROPIC POLYMERS

In the world of technology, polymers are used to the greatest extent in their isotropic form. They may be glassy and amorphous, like polystyrene, or

semicrystalline, like polyethylene, but in both cases they are used most frequently in the bulk isotropic forms. If science is to serve technology, one aim of the work with which we have dealt to date must be to predict or explain the stiffness of isotropic polymers. To what extent has this aim been fulfilled?

A brief consideration of the subject shows that it is made up of two problems. In the first place there is the problem of accounting for the stiffness of amorphous polymers, where we are handicapped by our lack of knowledge of the fine structure. More precisely, as with inorganic glasses, we lack a language to describe the structure because we lack the tools to elucidate it. Newer techniques such as small angle x-ray and long wavelength neutron scattering may be quite valuable here.

Another problem arises when dealing with semicrystalline polymers. We may regard them for many purposes as composite materials, made up of an amorphous phase and a polycrystalline phase. This is a crude but convenient picture, since it enables the basic concepts underlying the science of composite materials to be used (see e.g. ref. 52). Given the geometrical arrangements of the two phases (and this clearly involves far more than a mere knowledge of volume fractions), and given the stiffness of these phases, the problem is to predict the stiffness of the material. Underlying this is therefore the subsidiary problem of calculating the average stiffness of the polycrystalline phase from the moduli of the crystals along the chain, and transverse to the chain.

(a) Isotropic amorphous polymers

With this introduction, we consider first the isotropic amorphous polymer. Stiff materials of this type have Young's moduli in practice of the order of 3–6 $\times$ 10^{10} dyne cm^{-2} (this is in the region of polystyrene and thermosets). It would be attractive to be able to calculate this from compressibility data. Consider the relationship between K (bulk modulus) ($=1/\beta$ where β is the compressibility), E (Young's modulus) and ν (Poisson's ratio) for an isotropic material. If

$$K = E/3(1 - 2\nu) \tag{3}$$

$$E = 3K(1 - 2\nu) \tag{22}$$

or

$$E = 3(1 - 2\nu)/\beta \tag{23}$$

Now β for stiff polymers is in the region of 0.15–0.3 $\times$ 10^{-10} dyne cm^{-2} and ν is of the order of 0.3. Substituting these values in equation 23 gives the Young's moduli of 3–6 $\times$ 10^{10} dyne cm^{-2} mentioned above. To use this equation predictively, however, we must be able to calculate β and ν from first principles. Whilst some progress has been made towards calculating β for polymers (e.g. ref. 56), very little work indeed has been done on Poisson's ratio ν. As far as the authors are aware, no work has been done on relating Poisson's ratio to structure. This remains an interesting *terra incognita* for research, a situation which appears to be true for other materials also.

Bowden[40] has made a direct approach to the problem of calculating the stiffness of an isotropic glassy polymer. Bowden's argument takes the following form. The modulus of van der Waals solids is of the order of 4 $\times$ 10^{10} dyne

cm^{-2} (e.g. the transverse modulus of polyethylene or the modulus of solid argon; it should be noted here, however, that there is evidence that the $E_{\perp}$ for polyethylene may be $>4 \times 10^{10}$ dyne cm^{-2}, see *Table 5*). If this is a value based on van der Waals forces for a crystalline solid the value will be lower for amorphous polymers since the chain packing is irregular. This leads to an average increase in interchain distance which will reduce the van der Waals forces to the point where the modulus will be $< 4 \times 10^{10}$ dyne cm^{-2}, in which case some other mechanism is required to account for measured moduli of 3–6 $\times 10^{10}$ dyne cm^{-2}. These higher values can be explained on the reasonable assumption that the extension of an isotropic amorphous polymer takes place by rotation about carbon–carbon bonds in the chain backbone. Such a mechanism would lead to a calculated modulus of 5.7 $\times 10^{10}$ dyne cm^{-2} for amorphous polyethylene (this is close to the value calculated by Dulmage and Contois for this mode of deformation[12].

Arguments such as these yield figures for Young's modulus of the right order. For further progress to be made, a better structural model of an amorphous polymer is required. There are signs that such a model may be developed (see e.g. ref. 57).

(b) Isotropic semicrystalline polymers

Turning to the problem of the isotropic semicrystalline polymer such as polyethylene, this can be formulated as follows

$$E_{pca} = f(E_{am}, E_{pc}, V_g) \tag{24}$$

where E_{pca} is the Young's modulus of the isotropic semicrystalline polymer, E_{am} is the Young's modulus of the amorphous phase, E_{pc} is the Young's modulus of the polycrystalline phase, V_g is a term to represent the volume fraction of one of the phases, and all other geometrical variables such as crystallite size which will affect the modulus.

Furthermore, it can be expected from Hill's theory[9] that

$$E_{(V)pc} > E_{pc} > E_{(R)pc} \tag{25}$$

where $E_{(V)pc}$ and $E_{(R)pc}$ are the Voigt and Reuss averages of the elastic behaviour of the crystallites. These averages are derived from the elastic theories of a randomly oriented arrangement of small crystals, developed by Voigt[58] and Reuss[59]. Voigt assumed uniform strain throughout the assemblage whilst Reuss assumed uniform stress. Expressions 24 and 25 imply that there will be no unique value of E_{pca} or E_{pc}. It is likely that each will fall between upper and lower bounds.

Davidse, Waterman and Wasterdijk[53] have examined experimentally the elastic modulus of semicrystalline polyethylene extrapolated to 100 per cent crystallinity. This yields a value which should correspond to E_{pc} in equations 24 and 25. In this particular example, they obtained a value of $E_{pc} = 5.05 \times 10^{10}$ dyne cm^{-2}. More recently Gray and McCrum[61] have used a theoretically justified extrapolation procedure to obtain the amorphous and crystalline shear moduli of linear polyethylene at a measuring frequency of 0.67 Hz. At $-190°C$ this method gave $E_{pc} = 13 \times 10^{10}$ dyne cm^{-2} assuming Poisson's ratio $= 0.3$. For comparison, it is worth recalling that $E_{\parallel}$ is of the order of 300 $\times 10^{10}$ dyne cm^{-2} and $E_{\perp}$ of the order of 5–10 $\times 10^{10}$ dyne cm^{-2}.

The enormous predominance of $E_{\perp}$ in the average can thus be clearly seen and emphasizes the need for a precise value in the crystalline regions.

In their paper[46], Odajima and Maeda treat the same problem from a theoretical point of view, using their calculated values for the elastic constants of the polyethylene crystal. From these, they calculated the Voigt and Reuss averages and obtained the following results for the polyethylene polycrystal.

Table 6. Young's modulus of polycrystalline polyethylene E_{pc}

	Reuss average		Voigt average		Experimental[53]
	Set I	Set III	Set I	Set III	
E_{pc}, 10^{10} dyne cm^{-2}	4.90	5.82	15.6	15.8	5.05

The distinction between Set I and Set III refers to the alternative force constants used in the theoretical calculation of elastic constants by Odajima and Maeda. It will be seen that in this particular case the experimental data support the Reuss average, which is based on the assumption of uniform stress. Another value which would be required to make use of the expression set out as equation 24 is E_{am}, the modulus of the amorphous phase. The problems associated with predicting a value of E_{am} are typified in the paper by Bowden[40] discussed earlier. They are further complicated by the fact that the amorphous phase in a semicrystalline polymer may be rubbery or glassy which means that E_{am} may vary within the range 10^9 to 10^{10} dyne cm^{-2}. According to Gray and McCrum[61] $E_{am} = 3.2 \times 10^{10}$ dyne cm^{-2} at $-190°C$ for polyethylene but decreases to 0.5×10^{10} dyne cm^{-2} at $-80°C$ because of a low temperature relaxation. The value for polyethylene is around 10^9 dyne cm^{-2}. However, values above and below this range will also be encountered. For example, Dulmage and Contois[12] assumed a value for E_{am} with their fibre-forming polymers of 2×10^{10} dyne cm^{-2}, this corresponding to the modulus of the bulk polymer in the unoriented and amorphous state.

Uncertainty over the value of E_{am} forms one of the main difficulties in calculating the Young's modulus of an isotropic semicrystalline polymer. This can be illustrated by reference to *Figure 15* which represents equation 11 graphically and which shows the upper and lower bounds for the modulus when combining two phases 1 and 2 (see e.g. ref. 52). Assume that E_1 represents the modulus of the polycrystalline material, which appears from Odajima and Maeda's calculations may be close to the Reuss average. E_2 represents the modulus of the amorphous phase. A material at X will have a modulus between A and B, close to the lower bound. The precise value will depend on the crystallite size as well as on the volume fraction. The effect of a reduction in modulus of the amorphous phase can be seen by comparing the bounds from point D with those from point C.

It has already been pointed out that the modulus of the amorphous phase may be increased by the process of orientation. There is also evidence that

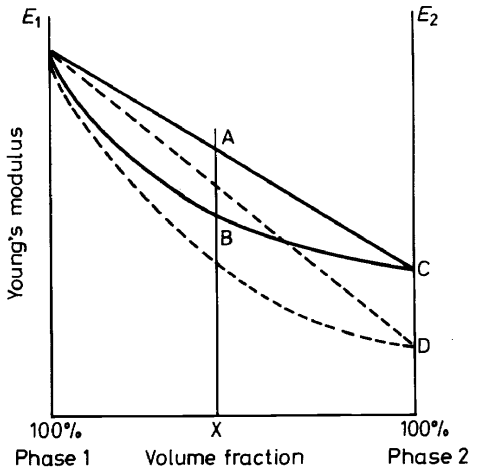

Figure 15. Upper and lower bounds of Young's modulus for a two-phase material.

the modulus of the amorphous phase may depend upon the degree of crystallinity. This appears from the work of Krigbaum, Roe and Smith[60] which is primarily directed towards a theoretical treatment of the modulus of semi-crystalline polymers, based on a refined statistical model. In this model, it is assumed that the process of crystallization places the remaining amorphous chains under considerable tension. If this model is correct, then E_{am} is effectively a function of the volume fraction of the crystalline phase—see equation 24. What is of equal significance to the present paper, is that Krigbaum *et al.* are able to calculate with reasonable accuracy the modulus of polyethylene based on modified statistical theory.

8. CONCLUSIONS

In dealing with the stiffness of polymers in relation to their structure, we have covered the range of Young's modulus from 10^9 to 10^{13} dyne cm^{-2}, this being the range from a soft amorphous polymer to the stiffness of graphite in the basal plane. Most attention has been devoted to the modulus of polymer crystals, along the chain and transverse to the chain. There is reasonable agreement between theory and practice in this case, and every reason to hope that further work will explain the discrepancies without fundamentally altering the picture, but possibly giving new data on the amorphous regions. The molecular modes of deformation have been clearly elucidated.

In passing from anisotropic to isotropic polymers the position becomes progressively more complex. Thus, theory adequately explains the stiffness along the chain in a polymer crystal, and with this as basis it is possible to account for the stiffness of highly oriented fibres, in which crystalline regions are effectively arranged in series with amorphous regions. The difference between the stiffnesses of different types of fibres is also readily explained in terms of the operative molecular modes of deformation. However, with

isotropic polymers, particularly the semicrystalline examples, the structural complexity of these materials makes model building difficult.

At the moment, it is possible to draw a line, at around an E value of 6×10^{10} dyne cm^{-2}, between isotropic and anisotropic polymers. Stiffness below this amount can be obtained in isotropic materials. Above this, use must be made of orientation to obtain the desired stiffness and results in excess of 10^{11} dyne cm^{-2} can be obtained. Where even higher stiffnesses are required, theory can suggest which modes of molecular deformation should be suppressed, and which relied upon.

REFERENCES

1. P. Vincent, *Proc. Roy. Soc. A*, **282**, 113 (1964).
2. See for example D. W. Hadley, P. R. Pinnock and I. M. Ward, *J. Materials Science*, **4**, 152 (1969).
3. M. J. P. Musgrave, *Crystal Acoustics*, Ch. 3. Holden-Day: San Francisco (1970).
4. G. J. Keeler and D. N. Batchelder, *J. Phys. Chem., Solid State Phys.* **3**, 510 (1970).
5. D. N. Batchelder, M. F. Collins, B. C. G. Haywood and G. R. Sidey, *J. Phys. Chem., Solid State Phys.* **3**, 249 (1970).
6. R. A. Cowley, W. J. L. Byers, E. C. Svensson and G. L. Paul, *Neutron Inelastic Scattering*, Vol. I, 281. I.A.E.A.: Vienna (1968); (relation of 'neutron' and 'ulrasonic' elastic constants).
7. C. P. Buckley, R. W. Gray and N. G. McCrum, *J. Polym. Sci.* **B7**, 835 (1969); **B8**, 341 (1970).
8. R. J. Samuels, *J. Polym. Sci.* **A3**, 1741 (1965).
9. R. Hill, *Proc. Phys. Soc. A*, **65**, 349 (1952).
10. I. Sakurada, T. Ito and K. Nakamae, *J. Polym. Sci.* **C15**, 75 (1966).
11. W. O. Baker and C. W. Fuller, *J. Amer. Chem. Soc.* **65**, 1120 (1943).
12. W. J. Dulmage and L. E. Contois, *J. Polym. Sci.* **28**, 275 (1958).
13. I. Sakurada, Y. Nukushina and T. Ito, *J. Polym. Sci.* **57**, 651 (1962).
14. I. Sakurada, T. Ito and K. Nakamae, *Makromol. Chem.* **75**, 1 (1964).
15. P. J. Hendra, *Laser Raman Spectroscopy*, Wiley: New York (1970).
16. R. F. Shauffele, *Trans. N.Y. Acad. Sci.*, Ser. II, **30**, No. 1, 69 (1967).
17. P. J. Hendra, *Advanc. Polym. Sci.* **6**, 151 (1969).
18. See for example J. W. White, *Excitons, Magnons and Phonons in Molecular Crystals*, p 43. Cambridge University Press: London (1968).
19. W. Cochran, *Rep. Progr. Phys.* **26**, 1 (1963).
20. See G. Dolling and A. D. B. Woods in P. A. Egelstaff, *Thermal Neutron Scattering*, pp 193, 200. Academic Press: New York (1965).
21. G. J. Stafford and A. W. Naumann, *Advance Polym. Sci.* **5**, 1 (1967).
22. S. Trevino and H. Boutin, *J. Macromol. Sci.* **A1**, 723 (1967).
23. G. F. Longster and J. W. White, *J. Chem. Phys.* **48**, 5271 (1968).
24. J. F. Twisleton and J. W. White, to be published in *J. Polym. Sci.*
25. J. W. White in *Textbook of Polymer Materials Science*, Ed. A. D. Jenkins.
26. L. A. Feldkamp, G. Venkateraman and J. S. King, *Neutron Inelastic Scattering* (Proceedings of a Symposium on Neutron Inelastic Scattering held at Copenhagen, May 1968), Vol. II, p 159, IAEA: Vienna (1968).
27. J. L. Koenig and F. J. Boerio, *J. Chem. Phys.* **50**, 2823 (1969).
28. V. La Garde, H. Prask and S. Trevino, *Disc. Faraday Soc.* **48**, 15 (1969).
29. C. P. Buckley and R. W. Gray, unpublished work.
30. D. H. C. Harris, S. J. Cocking, P. A. Egelstaff and F. J. Webb, *Inelastic Scattering of Neutrons in Solids and Liquids*, Vol. I, p 107. IAEA: Vienna (1963).
31. L. C. Bunce, D. H. C. Harris and G. C. Stirling, *UKAEA Res. Rep. No. 26246*, H.M.S.O.: London (1970).
32. R. M. Brugger in *Thermal Neutron Scattering*, Ch. 2. (Ed. P. A. Egelstaff). Academic Press: New York (1965).
33. W. L. Carrick, R. W. Kluiber, E. F. Bonner, L. H. Wartman, F. M. Rugg and J. J. Smith, *J. Amer. Chem. Soc.* **82**, 3883 (1960).
34. S. J. Cocking and Z. Guner, *Inelastic Scattering of Neutrons in Solids and Liquids*, Vol. I, p 237. IAEA: Vienna (1963).

[35] M. Lomer and G. G. E. Low, *Thermal Neutron Scattering*, Ch. 1. (Ed. P. A. Egelstaff). Academic Press: New York (1965).
[36] K. H. Meyer and W. Lotmar, *Helv. Chim. Acta*, **19**, 68 (1936).
[37] W. J. Lyons, *J. Appl. Phys.* **29**, 1429 (1958); **30**, 796 (1959).
[38] L. R. G. Treloar, *Polymer, London*, **1**, 95,279 and 290 (1960).
[39] E. Bartholomé and E. Teller, *Z. Phys. Chem. Lpz.* **B19**, 366 (1932).
[40] P. B. Bowden, *Polymer, London*, **9**, 449 (1968).
[41] S. Mizushima and T. Shimanouchi, *J. Amer. Chem. Soc.* **71**, 1320 (1949).
[42] R. F. Shauffele and T. Shimanouchi, *J. Chem. Phys.* **47**, 3605 (1967).
[43] J. W. White, *J. Macromol. Sci., Chem.*, **4**, 1275 (1970).
[44] T. Shimanouchi, M. Asahina and S. Enomoto, *J. Polym. Sci.* **59**, 93 (1962).
[45] M. Asahina and S. Enomoto, *J. Polym. Sci.* **59**, 101 (1962); **59**, 113 (1962).
[46] A. Odajima and T. Maeda, *J. Polym. Sci.* **C15**, 55 (1966).
[47] M. Tasumi, T. Shimanouchi and T. Miyazawa, *J. Molec. Spectrosc.* **9**, 261 (1962).
[48] J. H. Schachtschneider and R. G. Snyder, *Spectrochim. Acta*, **19**, 117 (1963).
[49] S. Enomoto and M. Asahina, *J. Polym. Sci.* **A2**, 3523 (1964).
[50] T. Miyazawa and T. Kitagawa, *J. Polym. Sci.*, **B2**, 395 (1964).
[51] R. G. Snyder, *J. Molec. Spectrosc.* **7**, 116 (1961).
[52] L. Holliday, *Composite Materials* (Ed. L. Holliday), Ch. 1. Elsevier: Amsterdam (1966).
[53] R. D. Davidse, H. I. Waterman and J. B. Wasterdijk, *J. Polym. Sci.* **59**, 389 (1962).
[54] A. H. Cottrell, *Proc. Roy. Soc. A*, **282**, 2 (1964).
[55] H. Matsuura and T. Miyazawa, *J. Polymer Sci.* **B7**, 65 (1969).
[56] R. N. Haward, *J. Polym. Sci.* **A2**, 7, 219 (1969).
[57] R. E. Robertson, *J. Phys. Chem.* **69**, 1575 (1965).
[58] W. Voigt, *Lehrbuch der Kristallphysik*, Teubner: Leipzig (1928).
[59] A. Reuss, *Z. Angew. Math. Mech.* **9**, 49 (1929).
[60] W. R. Krigbaum, R. J. Roe and K. J. Smith Jr, *Polymer, London*, **5**, 533 (1964).
[61] R. W. Gray and N. G. McCrum, *J. Polym. Sci.* **A2**, 7, 1329 (1969).